Open access Journal International Journal of Emerging Trends in Science and Technology

Negative Stiffness Structure for a Vehicle seat

Authors
Anita V. Hase, Tushar B Shinde, Ganesh Bhalerao
Department of Mechanical Engineering, SVCET, Rajuri
Pune, Maharashtra-412409, India

ABSTRACT
In this paper, an active pneumatic vibration isolation system using negative stiffness structures (NSS) for a vehicle seat in low excitation frequencies is proposed, the negative stiffness structures (NSS) are used to minimize the vibratory attraction of a vehicle seat. Thus, an adaptive intelligent back stepping controller (AIBC) is designed to manage the system operation for high-isolation effectiveness. In addition, an auxiliary control effort is also introduced to eliminate the effect of the unpredictable perturbations. Moreover, a radial basis function neural network (RBFNN) model is utilized to estimate the optimal gain of the auxiliary control effort.
The vibration isolator using a novel magnetic spring with negative stiffness (MS-NS) is proposed in this paper. The proposed isolator which combines a positive stiffness spring with the MS-NS in parallel possesses the characteristic of high-static–low-dynamic stiffness. The MS-NS is composed of three cuboidal magnets configured inrepulsive interaction. Ananalytical expression of the stiffness of the MS-NS is derived by using the magnetic charge model, and the approximation to the exact analytical expression is sought. Then, the nonlinearity of the stiffness Is analyzed, and it is shown that the MS-NS is approximately linear for small oscillations.

Introduction

As investigated by Paddan[1], unpleasant vibratory motion, which is distributed in low-frequency areas (0.5–5 Hz), are the main risk factors for lumbago or backache, which seriously affect the mental and physical health of drivers and passengers and reduce their working efficiency. Thus, to improve the ride comfort of passengers, seat vibration isolation systems should minimize these motions. However, with a conventional system, which includes a positive stiffness spring in parallel with a positive damping, it is difficult to isolate low-frequency vibrations. Therefore, currently, many researchers tried to offer solutions for this issue. Virginetal. [2,3] studied a thin strip as a nonlinear spring for supporting the load and mitigating the transmissibility of a dynamic vertical excitation. This strip is bent such that the two ends are brought together and clamped to form a teardrop shape. By increasing the loop length, the loop becomes less stiff vertically. As a result, one can achieve a low resonance frequency. Likewise, Chinetal. [4] considered the application of buckled columns as a vibration isolator having a softening spring. Pautetal. [5] studied the application of pairs of pre-columns bonded with a viscoelastic filler as a vibratory isolator. Hostensetal.[6] analyzed the vibratory isolator, which includes air spring and air damping.The result is to obtain a vibratory attenuation for low input frequencies and no linkage friction exists. However, a disadvantage of this system is that the extra air volume is too large. du Plooy et al. [7] developed a tunable vibratory absorbing isolator. In this system, a liquid inertia vibratory eliminator, which employs hydraulic fluid as the

vibratory absorber mass, is incorporated in the isolator. The stiffness, absorber mass, and port and reservoir geometry can be used to tune the absorber. Besides, Carrella et al. [8,9] proposed useful vibratory isolation models, which comprises a negative stiffness structure in parallel with the positive stiffness structure. Owing to the contrary effects of the negative and positive stiffness structures, the result is to achieve low dynamic stiffness. In addition, another mechanism with negative stiffness was designed by Lee et al. [10] to improve a railroad vibratory isolation system subjected to hazardous frequency vibrations.

With the improvement of accuracy of ultra-precision manufacturing and measuring equip-ment, the requirements for vibration isolation have become increasingly stringent [11–13]. Lowering the natural frequency of the isolator and introducing active control are two effective approaches for meeting these requirements. Absolute velocity feedback control creates 'sky-hook' damping to reduce the resonance peak effectively, but it cannot suppress the vibration at higher frequencies [14]. Feed forward control shows a significant effect against the direct disturbance of the machine on the isolated platform [15,16]. Reducing the stiffness of an isolator decreases its natural frequency, which will increase the band width of vibration isolation. However, low stiffness of the isolator using a linear spring causes large static deflection. Other methods should be used to lower the stiffness of an isolator. A vibration isolator which combines a positive stiffness spring with a negative stiffness element can support a large load statically while having small dynamic stiffness [17]. There are several ways to obtain this characteristic. Virgin [18] proposed a mechanism using extreme geometric nonlinearity, and it is based on a slender strip deformed at ear-shaped loop. Platus [19] proposed a negative-stiffness mechanism (NSM) based on the buckling of pre-stressed bars, and a vibration isolation system using the NSM was designed to obtain a lower naturals frequency.

Proposed system design concept

A Structure with Negative Stiffness:

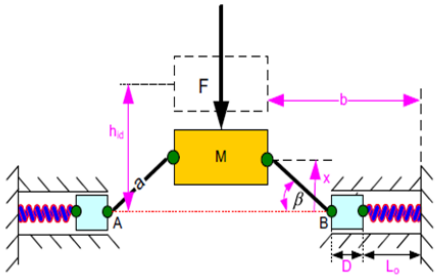

Figure No.01 Negative stiffness structure

Negative stiffness structures are shown diagrammatically in above figure. For the instant when the mass is displaced by some arbitrary amount from the initial position due to the action of force F that opposes the displacement. The result those two horizontal springs are compressed and generate two vertical restoring forces acting on the mass;

$$F = 2K_h\left(\frac{L_0}{\sqrt{a^2 - x^2}} - \frac{b}{\sqrt{a^2 - x^2}} + 1\right)x \qquad (1)$$

It is convenient to define the following dimensionless parameters:

$$\hat{F} = \frac{F}{K_h L_o}, \hat{x} = \frac{x}{L_o}, \gamma_1 = \frac{a}{L_o}, \gamma_2 = \frac{b}{L_o} \qquad (2)$$

Where,

$\hat{F}$ = Dimension less restoring force,

$\hat{x}$ = Dimensionless displacement of the mass relative to the base,

γ_1 and γ_2= The configurative parameters,

a = The length of the bar,

b= The distance from the wall to the mass,

K_h =Stiffness,

$L_{o=}$ Original length of the horizontal spring,

$$\hat{F} = 2\left(\frac{1}{\sqrt{\gamma_1^2 - \hat{x}^2}} - \frac{\gamma_2}{\sqrt{\gamma_1^2 - \hat{x}^2}} + 1\right)\hat{x} \qquad (3)$$

Above figure show the parametric dependence between the dimensionless restoring force $\hat{F}$ and the dimensionless displacement $\hat{x}$.

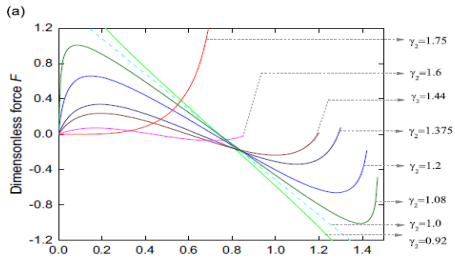

Figure No. 02 (a). Dimensionless force-deflection characteristics

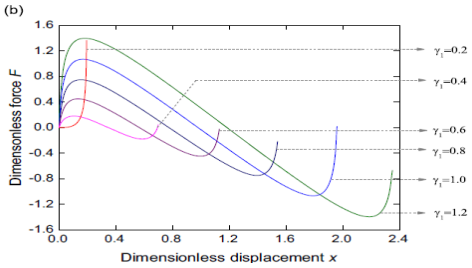

Figure No.02 (b). Dimensionless force-deflection characteristics

In this figure some predictions in the design of a negative stiffness structure. The first case is if the value $\gamma_2 < 1$, the restoring force curves always decreases the displacement increases. In this case, the structure derives the negative stiffness but this condition will not be considered for designing a negative stiffness structure of the proposed model. If the values, $1 \le \gamma_2 < 1.75$, The restoring force exists the maximum and minimum forces at the location of the mass $\hat{x}_1$ and $\hat{x}_2$ respectively.

The second case is shown in figure indicates the values of $\gamma_1 \ge 0.2$ it is similar to the first case values $1 \le \gamma_2 < 1.75$; the system also has displacement intervals with negative stiffness. When the values of $\gamma_1 \le 0.2$, the system cannot work as the negative stiffness structure, because the stiffness of the structure is always positive.

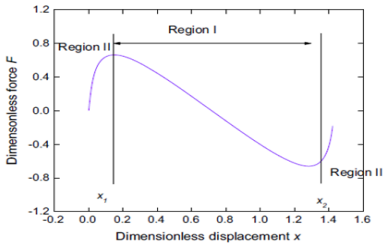

Figure No. 03. Region of negative and positive stiffness

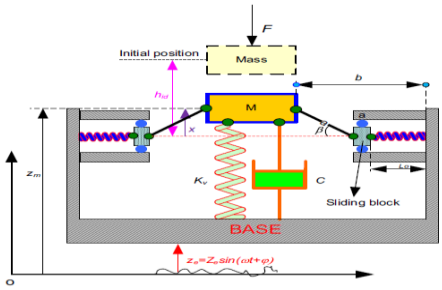

Figure No.04. Mechanical model of the passive isolation system

Based on NSS, We design a passive system with NSS shown in fig.4. This system can give a low dynamic stiffness. The passive system with NSS has higher isolation effectiveness than the passive system without NSS shown following figure.

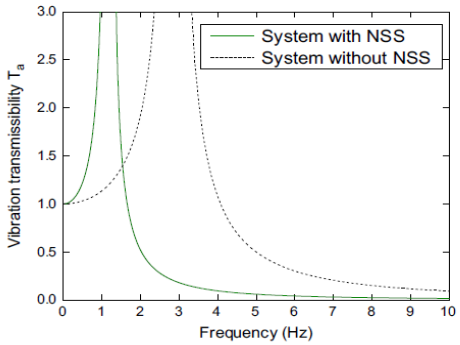

Figure No.05.Comparisons of vibration transmissibility between system with NSS & without NSS.

Active System with NSS:

The simple vehicle seat mode comprises an isolation system, a seat frame, and a human body, for our analysis, the weight, elasticity and stiffness of the seat cushion and the damping of the components inside of a human body, such as the spine, are all ignored.

The active system with NSS is shown in Fig. 6. The model comprises the negative stiffness structure in parallel with a load support spring (vertical spring) having positive stiffness, a damper and a low-friction pneumatic cylinder directly controlled by a proportional valve. As in the above analysis, the active system with NSS offers a low stiffness; thus it reduces attraction of the vibration force.

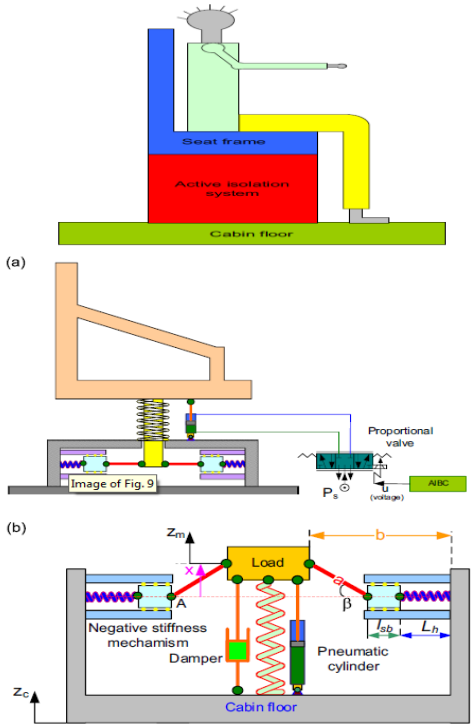

Figure No.06.Vibratory isolation seat model using negative stiffness structure (a), & mechanical model of isolation system (b)

Experimental Apparatus:

To investigate the control performance of the active system using NSS, an experimental apparatus is built having the configurative parameters listed in Table 1. According to the values of these parameters, the dynamic stiffness curve of the proposed system is depicted as in Fig.7. It can be seen that around the static equilibrium position, the dynamic stiffness of the system is very low and at this position, the dimensionless dynamic stiffness value is nearly equal to 0.23. It means that the dynamic stiffness is nearly equal to 0.23 times the static stiffness of the system.

The hardware of the experimental model is shown in Fig. 8, including the main spring for bearing the load, the low friction pneumatic cylinder installed between the cabin floor and the mass and directly controlled by a proportional valve, the NSS to reduce the vertical dynamic stiffness of the system and a vibration exciter manufactured by Park electric. In addition, a laser sensor and an accelerometer are installed to observe the vertical displacement and acceleration of the mass.

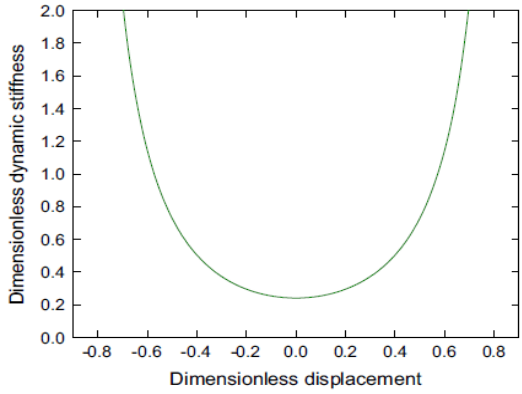

Parameter	Original value
a	187 mm
b	370 mm
K_h	600 N/mm
K_v	800 N/mm
M	4.5 kg

Table 01 Dimensionless dynamic stiffness curve

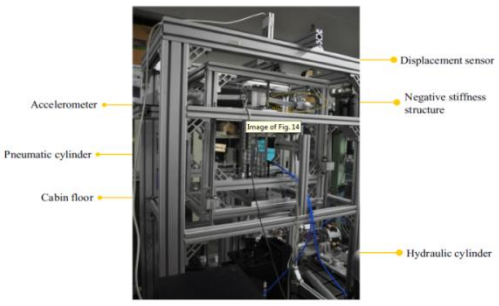

Fig 08.The experimental apparatus

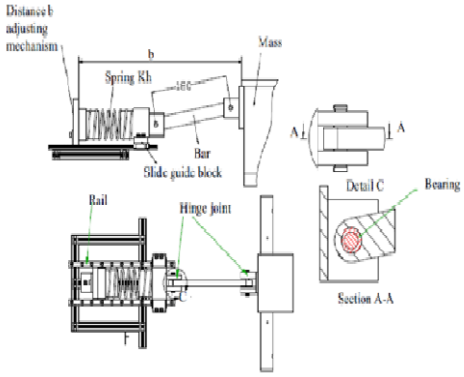

Fig. 09. Details of negative stiffness element

Experimental Results

The control algorithm is designed by a combination of Simulink and the real-time Windows Target Toolbox of MATLAB. Fig.10 displays the overall control scheme of the active system using the AIBC. The Simulink block reads the absolute displacement of the mass through the laser sensor and calculates the voltage to be supplied to the proportional valve.

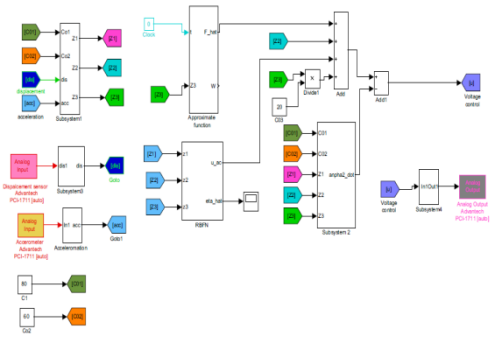

Fig.10. Overall control scheme of the active system using AIBC

Sinusoidal Excitation:

When the cabin floor is excited by a sinusoidal wave with an amplitude of 15mm and a frequency of 0.8 Hz, the mass position response is presented in Fig.11. The dashed line exhibits the excitation signal, the solid line is used to denote the mass position response controlled by the BC with a fixed gain of the auxiliary effort and the solid-bold is used to depict the mass displacement response controlled by AIBC. It can be seen that the AIBC performs slightly better than the BC. The root mean square (RMS) is 0.867 mm and 1.2675 mm for the AIBC and BC, respectively.

Besides, the estimated values of the unknown function f(y,t) based on the approximate technique are shown in Fig.12.

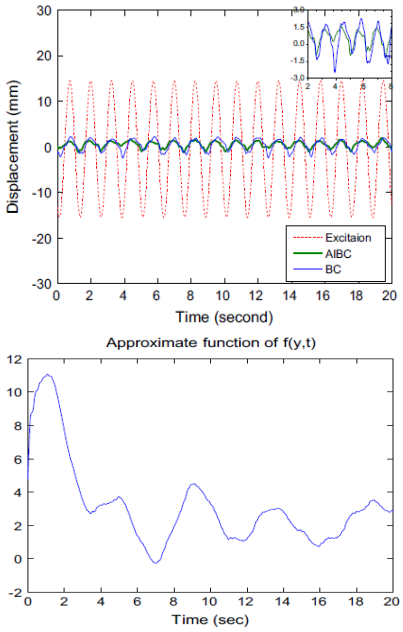

Fig 11. Time history of mass displacement fig 12 Approximation of function f(y,t).

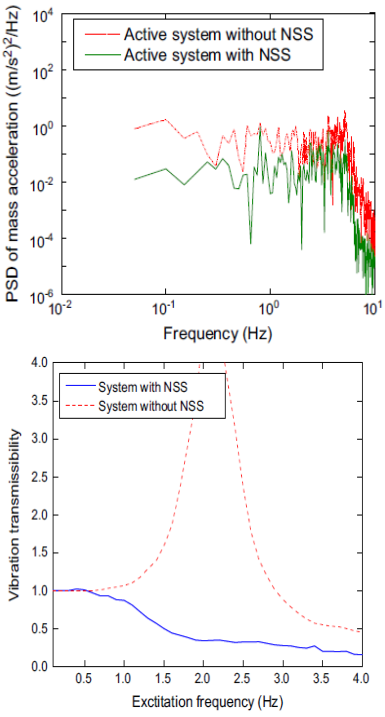

Fig. 13. Response of the mass acceleration. Fig.14. Frequency response comparison

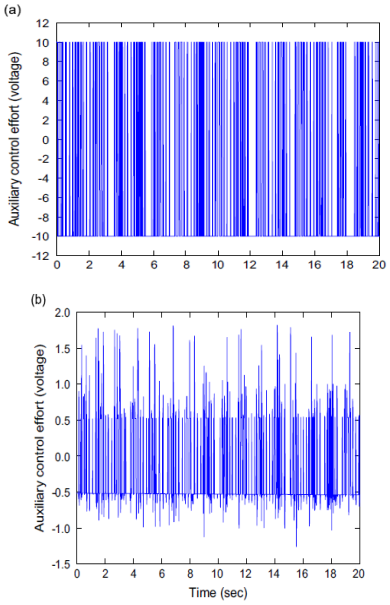

Fig. 15 Auxiliary control signal under sinusoidal excitation: (b)BC; (a)AIBC

Fig. 13 shows the comparison of the isolation performances between the active system with NSS and the active system without NSS . Both the systems are controlled by the AIBC. The solid line denotes the active system with NSS, and the other line represents the active system without NSS. It can be seen that the PSD value of the mass acceleration isolated by the active system without NSS is lower than that of the excitation signal at 0.8Hz (10^2 $(m/s^2)^2$). However, the PSD value of the mass acceleration of the introduced system is smaller than that of the mass acceleration of the active system without NSS. This concludes that the active system with NSS suppresses the vibrations from the base more effectively than the active system without NSS. As shown in Fig.09, the dynamic stiffness of the system with NSS is nearly equal to 0.23 times the stiffness of the system without NSS at the static equilibrium position. Hence, the isolation range of the passive system with NSS is larger than that of the passive system without NSS as shown in Fig.14. It can be seen that the passive system with NSS can isolate vibrations having the frequency greater than 0.5Hz, whereas by using the passive system without NSS, the vibration attenuation can only occur for the excitation frequency greater than 3Hz.For frequencies less than 3Hz,the passive system without NSS attracts vibration force strongly. Besides, it also confirms that the passive system with NSS has a higher vibratory attenuation rate than the passive system without NSS. It indicates that vibratory attraction of the system without NSS is higher than that of the system with NSS.

Bump Excitation:

In this case, the isolation performance of the active system using NSS is assessed by a bump excitation having a maximum heightof15mm.The time history of the mass acceleration using the AIBC and BC is presented in Fig.16. It can be seen that the isolation efficiency of the AIBC is better than that of the BC. In this case, the maximum acceleration of the mass for using the AIBC and BC is 0.4 m/s^2 and 0.8m/s^2, respectively. The RMS values of the mass displacement are 0.237mm for the AIBC and 0.4897 for the BC.

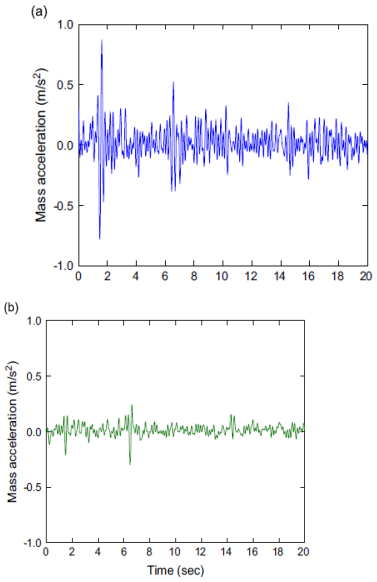

Fig. 16. Time history of the mass acceleration using (a) BC and (b) AIBC.

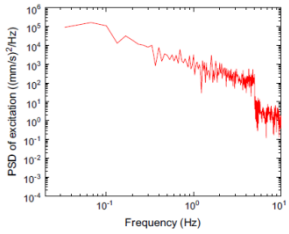

Fig. 17. PSD of excitation.

Random Excitation:

A random excitation is used to compare the isolation performance of the active system with NSS controlled by the AIBC and the BC. The power spectrum density (PSD) is described in Fig.17. It reveals that excitation frequency range is mainly spread within0.1–10Hz. The result is the mass displacement response depicted in Fig. 18. Here, the dashed line, solid line and solid bold line represent the excitation, the mass position response using the BC and the AIBC, respectively. It can be observed that the RMS of the mass displacement is reduced from1.01mm to 0.66mm by introducing AIBC. Fig. 19 shows the PSD of the mass acceleration. The dashed line exhibits them as acceleration using the BC and the solid line depicts the acceleration using the AIBC. It is seen that within 0.1–10Hz, the isolation performance of the AIBC is improved more effectively than the BC.

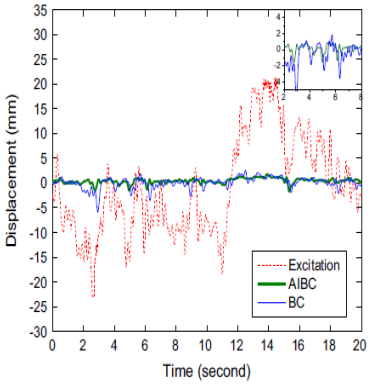

Fig. 18. The mass position variation with respect to time.

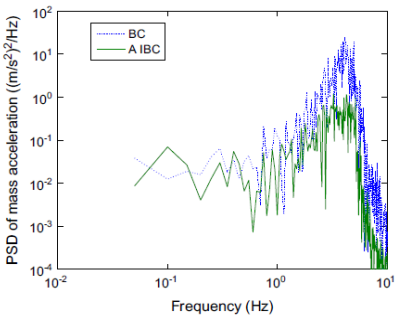

Fig. 19. Power spectrum density of mass acceleration.

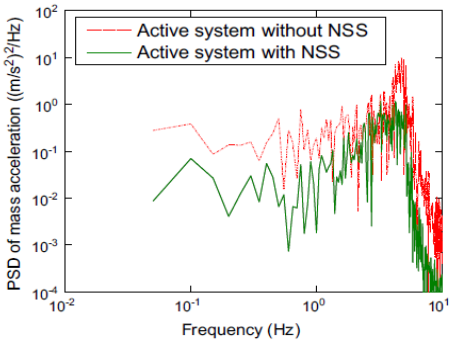

Fig. 20. Comparison of PSD of mass acceleration with and without NSS.

In addition, the same above random excitation, Fig.20 shows the comparison of the vibratory performance between the active system with NSS (solid line) and the active system without NSS (dashed line). Both systems are controlled by the AIBC. It can be observed that the vibratory attraction of the active system without NSS is higher than that of the active system with NSS, and the isolation performance of the active system with NSS is better than that of the active system without NSS.

Magnetic spring with negative stiffness:

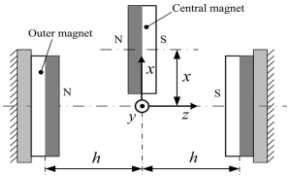

Fig. 21. Schematic of the MS-NS.

The MS-NS is depicted in Fig. 21. It consists of three cuboidal magnets magnetized in the z-direction. The central magnet and the outer magnets are configured in repulsive interaction. It is assumed that the central magnet can move only in the x-direction. The other degrees of freedom will be constrained by applying extra mechanism, such as a flexible hinge. The central magnet acts as a spring with negative stiffness. The stiffness of the magnetic spring attributes to magnetic force. It can be adjusted by changing the distance h between the central magnet and the outer magnets.

Passive vibration isolator

Structure of the vibration isolator:

The proposed vibration isolator which combines a positive stiffness spring with the MS-NS in parallel is depicted in Fig. 22 the movement of the load is guided by two flexible hinges. The positive stiffness spring contains a coil spring and the two flexible hinges which also should be seen as a spring. The stiffness of the MS-NS can be adjusted to obtain lower natural frequency. The central magnet is held by an aluminum box which is connected with the load by a screw. And the total load is supported by the coil spring. To reduce the influence on the magnetic field, most parts of the isolator are manufactured with stainless steel or aluminum materials.

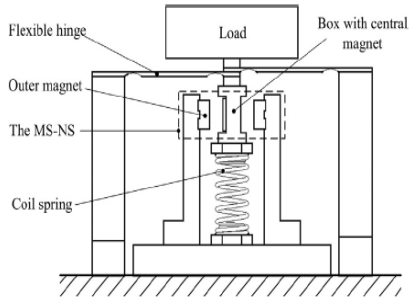

Fig.22. Schematic diagram of the developed vibration isolator.

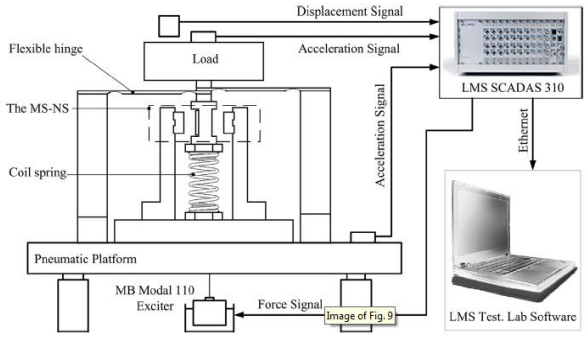

Fig. 23. The sketch of the experimental set-up.

Models of the vibration isolator

The relationship between the applied force f acting on the load and the relative displacement x can be derived as:

$$f = k_p x + k_1(h)x + \frac{k_2(h)}{3}x^3$$

where kp is the stiffness of the positive stiffness spring.

The total stiffness of the isolator can be obtained by differentiating f with respect to x, which is given by,

$$k = k_p + k_1(h) + k_2(h)x^2$$

In Fig. 22, the vibration isolator is mounted on the floor. The load vibrates due to the micro-vibration from the floor. With effect of the flexible hinges, the load can move only in the vertical direction translationally. And it is reasonable that the isolator can be treated as a single-degree-of-freedom model. The equation of motion for the isolator is given by

$$m\ddot{x}_1 + (c_p + c_n)(\dot{x}_1 - \dot{x}_0) + (k_p + k_n)(x_1 - x_0) = 0$$

where m is the mass of the total load, x_0 and x_1, respectively, are the displacement of the floor and the load, c_p and c_n are the damping of the positive stiffness spring and the MS-NS separately, k_p and k_n are the stiffness of the positive stiffness spring and the MS-NS respectively.

The transfer function representation of the dynamics can be expressed as,

$$T(s) = \frac{x_1(s)}{x_0(s)} = \frac{(c_p + c_n)s + (k_p + k_n)}{ms^2 + (c_p + c_n)s + (k_p + k_n)}$$

in which $x_0(s)$ and $x_1(s)$ are the Laplace transform of the input and output signals, respectively.

Experiments

Set-up of experiments

The passive vibration isolator described in Fig.22 is designed to illustrate the principle and validate the analysis of the MS-NS. The stiffness of the MS-NS can be adjusted by adjusting the distance of the outer magnets during the experiments. The sketch of experimental set-up is shown in Fig. 23.

Experimental results

Six groups of experiment are carried out in this research. In experiments 1 and 4,the outer magnets of the MS-NS are removed, and then the vibration transmissibility of the isolator without the MS-NS is measured. The stiffness and the damping of the positive stiffness spring are identified as known parameters by using the test results inexperiment1. In experiments1–3, the isolated load is 1.35 kg. The isolated load is varied in experiments 4–6 to make the experimental results more convincing. Mean while, for the purpose of validating the effectiveness and correctness of the MS-NS, the isolator with the MS-NS is studied in different conditions. The distance h is designed as 17 mm in experiments 2 and 5 (the measured value is 17.08 mm and 17.04 mm in experiments 2 and 5 respectively), and 14 mm in experiments 3 and 6 (the measured value is 14.05 mm and 14.17 mm in experiment 3 and 6 respectively). The distance h between the outer magnets and the central magnet is half of the gap between the outer magnets plus the thickness of an outer magnet. Given that the static displacement of the isolated load is due to gravity and in order to ensure the MS-NS operates around the expected initial position, two thin washers of about 1 mm are attached on the two sides of the coil spring when the isolated load is 1.35 kg. And when the isolated load is 2.29 kg, three thin washers are used. Also, when the isolated load is removed, the thin washers are taken off at the same time.

Stiffness and damping estimated in the experiments, the natural frequency in experiment and calculation.

Experiment times	Stiffness(Nm^{-1})	Damping($Nm^{-1}s$)	Frequency (Hz)	Frequency (calculation)
Experiment 1	9638	2.164	13.43	-
Experiment 2	5965	2.031	10.55	9.961
Experiment 3	1964	2.258	6.07	5.664
Experiment 4	9872	2.216	10.45	10.325
Experiment 5	5543	2.198	7.83	7.564
Experiment 6	2224	2.165	4.96	4.566

In this study, we make sure that the isolator operates in the expected initial position as much as possible by structural design and adding thin washers on the two sides of the coil spring to compensate size error and gravity of the load. The errors of analytical results and tests results partly come from this factor. Assuming that the isolator operates in the expected initial position, the static displacement is dependent only on the positive coil spring, which has a stiffness of 9638 N/m resulting in a static displacement of only 1.38 mm at a load of 1.35 kg. A linear spring with a coefficient of 1964 N/m will have the same natural frequency of 6.07 Hz at the same load, but it results in a static displacement of 6.78 mm.

CONCLUSIONS

First, the negative stiffness structure was analyzed in detail, and an active pneumatic vibration isolation system using negative stiffness structure was proposed. Then, an AIBC was designed and successfully employed for the proposed system. In addition, an auxiliary controller was introduced to eliminate the effect of the unpredictable perturbations. Besides, the RBFNN model was used to estimate the optimal gain of the auxiliary controller reduce the chattering phenomenon in the control effort. Then, the experiments are realized to assess the vibratory performance of the active system with NSS managed by the proposed AIBC. The experimental results confirmed that the isolation effectiveness of the active system

with NSS is upgraded compared with that of the active system without NSS. Although the proposed system has time-varying and non linear behavior, experimental results indicated that the AIBC is an effective solution for the proposed system.

The vibration isolator which combines a coil spring in parallel with a novel MS-NS is proposed in this paper. The MS-NS consists of three magnets configured in repulsion, and it is modeled using magnetic charge model. Approximation to the analytical model is sought. With the established model, the nonlinear behavior of the stiffness is discussed. The vibration transmissibility of the vibration isolator is calculated. During the experiments, the stiffness of the MS-NS is adjusted to validate the analytical calculation. The natural frequency of the isolator with a load of 1.35 kg is reduced to 6.07 Hz by using the MS-NS, while the resonance frequency of the isolator without the MS-NS is about 13.43 Hz. At a different load of 2.29 kg, the natural frequency of the isolator is reduced from 10.45 Hz to 4.96 Hz. It demonstrates that the proposed isolator using the MS-NS can realize low-frequency vibration isolation without increasing the static deflection of the isolator. Consequently, this type of vibration isolator is suitable for applications on ultra-precision manufacturing and measurement equipment. Meanwhile, the analytical results are consistent with the experimental results. It indicates that the analytical expression of the stiffness of the MS-NS can be used for stiffness optimization of the MS-NS.

References

1. G.S. Paddan, M.J. Griffin, Evaluation of whole-body vibration in vehicle, Jou. of Sound & Vibration 253 (1)(2002)195–213.
2. L.N. Virgin, S.T. Santillan, R.H. Plaut, Vibration isolation using extreme geometric nonlinearity, Journal of Sound and Vibration 315(3)(2008)721–731
3. S. Santillan, L.N.Virgin, R.H.Plaut, Equilibria and vibration of a heavy pinched loop, Journal of Sound and Vibration 288 (1–2) (2005)81–90.
4. E.J. Chnin, K.T. Lee, J. Winter flood, L.Ju, D.G.Blair, Low frequency vertical geometric anti-spring vibration isolators, Physics Letters A 336(2–3) (2005) 97–105.
5. R.H. Plaut, H.M.Favor, A.E.Jeffers, L.N.Virgin, Vibration isolation using buckled or prebent columns- part1: two-dimensional motion of horizontal rigid bar, Journal of Sound and Vibration 310 (1–2) (2008) 409–420
6. I. Hostens, K.Deprez, H.Ramon, An improved design of air suspension for seats of mobile agriculture machines, Journal of Sound and Vibration 276(1–2) (2004)141–156.
7. N.F.duPlooy,P.s.Heyns,M.J.Brennan,Thedevelopmentofatunablevibrationabsorbingisolator, International Journal of Mechanical Sciences 47(7) (2005)983–997.
8. A.Carrella, M.J.Brennan, T.P.Waters, Static analysis of a passive vibration isolation with quasizero- stiffness characteristic, Journal of Sound and Vibration 301(3–5) (2007)678–698.
9. A.Carrella, M.J.Brennan,T.P.Waters,K.Shin,Onthedesignofa high-static-low-dynamic stiffness isolator using linear mechanical springs and magnets, Journal of Sound and Vibration 315(3) (2008)712 –720.
10. C.-M. Lee, A multistage high speed rail road vibration isolation system with “negative” stiffness, Journal of Sound and Vibration 331(4)(2012)914–921.
11. C.G. Gordon, Generic vibration criteria for vibration-sensitive equipment, Proceedings of SPIE, SanJose, CA,1999
12. E.H Anderson, B. Houghton, ELITE-3 active vibration isolation workstation, Proceedings of SPIE, 2001, pp.183–196.

13. Y. -H. Shin, K. -J. Kim, Performance enhancement of pneumatic vibration isolation tables in low frequency range by time delay control, Journal of Sound and Vibration 321(2009)537–553.
14. B. Yan, M.J .Brennan, S.J. Elliott, N.S. Ferguson, Active vibration isolation of a system with a distributed parameter isolator using absolute velocity feedback control, Journal of Sound and Vibration 329 (2010)1601–1614
15. M.Y asuda, T. Osaka, M. Ikeda, Feed forward control of a vibration isolation system for disturbance suppression, Proceedings of the 35th IEEE Decision and Control, IEEE,1996,pp.1229–1233.
16. T.H. Yan, H.Y. Pu, X.D. Chen, Q.Li, C.Xu, Integrated hybrid vibration isolator with feed forward compensation for fast high-precision positioning X/ Y tables, Measurement Science and Technology 21 (2010) 065901.
17. A.Carrella, M.J.Brennan, T.P.Waters, K.Shin, On the design of a high-static–low-dynamic stiffness isolator using linear mechanical springs and magnets, Journal of Sound and Vibration 315(2008)712–720.
18. L. Virgin, S.Santillan, R.Plaut, Vibration isolation using extreme geometric nonlinearity, Journal of Sound and Vibration 315(2008)721–731
19. D. L. Platus, Negative-stiffness-mechanism vibration isolation systems, Proceedings of SPIE, 1991, pp. 44–54.